Colloids and Surfaces B: Biointerfaces 267 (2026) 115925

Contents lists available at ScienceDirect

Colloids and Surfaces B: Biointerfaces

journal homepage: www.elsevier.com/locate/colsurfb

A photothermally addressable Tomato extracellular vesicle-integrated polypyrrole/gellan gum hydrogel for microenvironmental reprogramming of diabetic wounds

Yao-Jen Chang [a,b], Yao-Wei Liou [c], Lekshmi Rethi [c], Sih-Chi Chuang [c], Pei-Chia Hung [d], Ching-Cheng Huang [e,f], Yi-Ting Shu [g,*], Jie-Fan Chang [a,*], Chiou-Shann Fuh [a,*], Andrew E.-Y. Chuang [c,h,i,**]

[a] Department of Computer Science and Information Engineering, National Taiwan University, Taipei 10617, Taiwan
[b] Department of Plastic Surgery, Shin-Kong Wu Ho-Su Memorial Hospital, Taipei, Taiwan
[c] Graduate Institute of Biomedical Materials and Tissue Engineering, College of Biomedical Engineering, Taipei Medical University, New Taipei City, Taiwan
[d] Hsuan Chen Technology Co., Ltd., New Taipei City 22055, Taiwan
[e] Department of Biomedical Engineering, Ming-Chuan University, Taoyuan city, Taiwan
[f] College of Science And Technology, Nanhua University, Chiayi, Taiwan
[g] Department of Materials and Textiles, Asia Eastern University of Science and Technology, New Taipe City, Taiwan
[h] International Ph.D. Program in Biomedical Engineering, College of Biomedical Engineering, Taipei Medical University, New Taipei City, Taiwan
[i] Cell Physiology and Molecular Image Research Center, Taipei Medical University-Wan Fang Hospital, Taipei 11696, Taiwan

ARTICLE INFO

Keywords:
Diabetic wound healing
Tomato-derived extracellular vesicles
Photothermal hydrogel
Microenvironment remodeling
Angiogenic regeneration

ABSTRACT

Chronic diabetic wounds remain difficult to treat because they are characterized by persistent oxidative stress, prolonged inflammation, impaired angiogenesis, and delayed tissue regeneration. Here, we report a smart TEV/PVA-PEI-PPY@GG hydrogel that integrates tomato-derived extracellular vesicles (TEV), a polypyrrole (PPY)-based near-infrared (NIR)-responsive photothermal component, and a gellan gum (GG) matrix for diabetic wound treatment. The engineered platform exhibited favorable colloidal stability, a porous and structurally integrated architecture, tunable mild photothermal responsiveness under 808 nm irradiation, and retained antioxidant activity associated with the vesicular fraction. In vivo, TEV/PVA-PEI-PPY@GG significantly accelerated wound closure, improved epidermal continuity, and enhanced dermal remodeling in streptozotocin-induced diabetic wounds, while showing no obvious histopathological toxicity in major organs. Immunohistochemical and histological analyses revealed altered expression patterns of AHR, TNF-α, CD31, and CD34 in treated tissues, which may contribute to tissue repair, modulation of inflammatory responses, and angiogenic remodeling during wound healing. These changes were associated with improved wound regeneration and restoration of tissue architecture. Overall, this work demonstrates the potential of a plant EV-integrated photothermally responsive hydrogel as a therapeutic strategy for diabetic wound repair and supports the possibility that local microenvironment modulation may contribute to its beneficial effects.

1. Introduction

Diabetic wounds are a major complication of diabetes, characterized by impaired healing due to oxidative stress, chronic inflammation, poor angiogenesis, and defective tissue remodeling [1-3]. Unlike acute wounds, they remain in a prolonged inflammatory state with reduced re-epithelialization and neovascularization, leading to delayed healing and increased risks of infection and tissue damage [2,4,5]. Therefore, effective therapies might not only provide wound coverage but also actively modulate the pathological microenvironment for promoting

* Corresponding authors.
** Corresponding author at: Graduate Institute of Biomedical Materials and Tissue Engineering, College of Biomedical Engineering, Taipei Medical University, New Taipei City, Taiwan.
E-mail addresses: fc020@mail.aeust.edu.tw (Y.-T. Shu), jfanc@ntu.edu.tw (J.-F. Chang), fuh@csie.ntu.edu.tw (C.-S. Fuh), eychuang@tmu.edu.tw (A.E.-Y. Chuang).

https://doi.org/10.1016/j.colsurfb.2026.115925
Received 2 April 2026; Received in revised form 30 May 2026; Accepted 18 June 2026
Available online 22 June 2026
0927-7765/© 2026 Elsevier B.V. All rights are reserved, including those for text and data mining, AI training, and similar technologies.

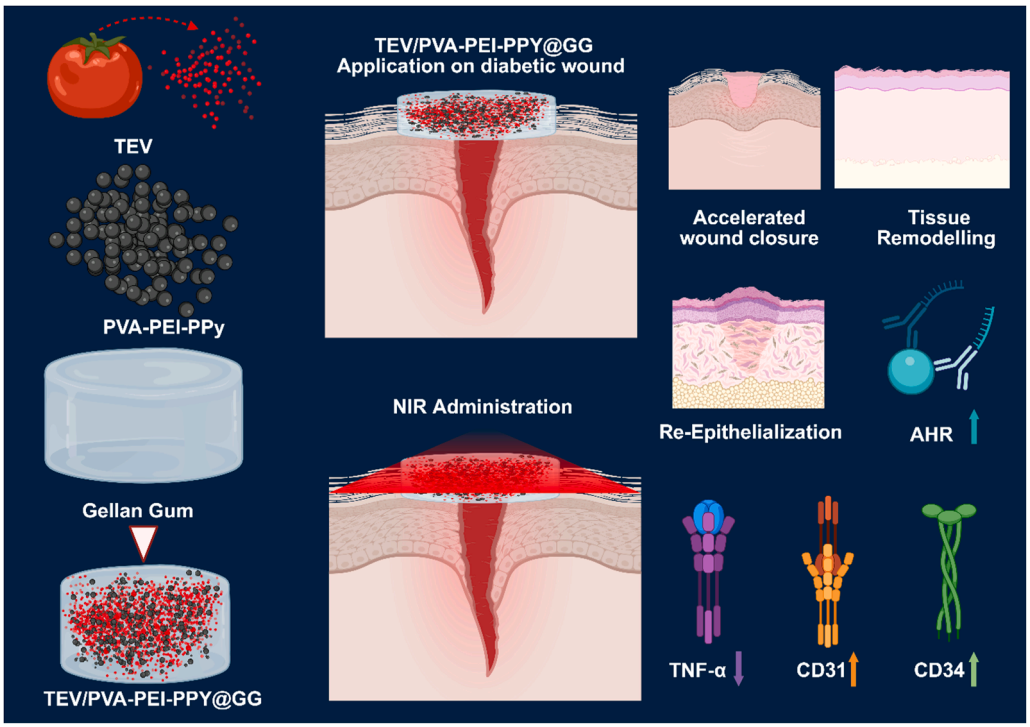

Scheme 1. The TEV/PVA-PEI-PPY@GG hydrogel is a multifunctional platform for diabetic wound repair, integrating plant-derived extracellular vesicles, an NIR-responsive PPY photothermal module, and a gellan gum matrix. Created in BioRender. Chuang, A. (2026) https://BioRender.com/4sxhtfo.

regeneration.

Biomaterial-constructed wound dressings, particularly hydrogels, have shown promise for diabetic wound alleviation due to their high-water content, tissue-like properties, and ability to conform to irregular surfaces, enabling moisture retention, exudate absorption, and delivery of bioactive substance [6-8]. Nevertheless, conventional hydrogels often act as passive carriers and lack the ability to actively modulate the wound environment. Thus, multifunctional systems that combine structural support with bioactive and controllable therapeutic bio-functions are increasingly needed [6,9,10].

Extracellular vesicles (EVs) are promising therapeutic agents because of their bioactivity and role in intercellular communication. Plant-derived EVs, in particular, offer advantages such as biocompatibility, accessibility, and inherent antioxidant as well as anti-inflammatory properties [11–13]. In this study, Tomato derived EVs (TEV) showed nanoscale size and antioxidant activity, indicating their potential for reducing oxidative stress and promoting a regenerative microenvironment in diabetic wounds [3,14,15].

Conductive photothermal polymeric materials have gained attention for their ability to convert NIR light into localized heat, enabling controlled as well as noninvasive modulation of tissue responses [16-18]. Polypyrrole (PPY), known for its stability and photothermal properties, was incorporated as PVA/PEI-PPY in this system, demonstrating NIR-responsive behavior. Beyond heat generation, it also contributes to polymeric hydrogel stability and enhances therapeutic responsiveness under external stimulation [19-25].

For further translating these bioactive and photothermal elements into a practical wound dressing system, gellan gum (GG) provides an appealing hydrogel matrix on account of its gel-forming capability, biocompatibility, and suitability for topical administration [26-30]. By integrating TEV and PVA/PEI-PPY into a GG-based hydrogel, it becomes possible to construct a multifunctional platform that combines bio-activity, physicochemical stability, and external NIR responsiveness. Such a composite system is expected to not only cover and protect the wound surface but also modulate the local lesion microenvironment through antioxidative support, inflammation attenuation, and enhanced tissue reconstruction.

Despite advances in hydrogel-based wound dressings, most currently reported systems primarily function as passive protective matrices and fail to simultaneously address the complex pathological features of diabetic wounds, including oxidative stress, persistent inflammation, impaired angiogenesis, and defective tissue remodeling. Although extracellular vesicles have demonstrated regenerative potential, their integration into stimuli-responsive hydrogel systems for controlled diabetic wound modulation remains limited. Similarly, conductive photothermal materials such as PPY have shown promise in externally regulated therapy; however, their combination with plant-derived EVs within a biocompatible hydrogel matrix has been insufficiently explored. Therefore, there remains a need for a multifunctional platform capable of integrating antioxidative bioactivity, photothermal responsiveness, and structural wound support into a single system for enhanced diabetic wound regeneration.

Herein, we developed a multifunctional TEV/PVA-PEI-PPY@GG hydrogel dressing that integrates plant-derived extracellular vesicle bioactivity with NIR-responsive conductive photothermal modulation within a GG hydrogel matrix. Unlike conventional passive wound dressings, this platform was designed to actively regulate the diabetic wound microenvironment through antioxidative activity, inflammation attenuation, and externally controllable photothermal stimulation. By combining the regenerative potential of TEV, the photothermal responsiveness of PPY-containing composites, and the biocompatibility of GG hydrogel, this system aims to promote enhanced tissue repair and wound regeneration. Its therapeutic potential was systematically evaluated through physicochemical characterization, photothermal assessment, and in vivo diabetic wound healing studies.

2. Experimental section

2.1. Materials and methods

2.1.1. Preparation and photo thermal evaluation of PVA/PEI-PPY photothermal nanocomposites

Polyvinyl alcohol (PVA, 1.5 g, Sigma Aldrich, USA) was dissolved in 15 mL of deionized water at 80 °C with continuous stirring. After cooling to room temperature, polyethyleneimine (PEI, 0.2 g, Sigma Aldrich, USA) was added, followed by pyrrole monomer (12.5 μL, Sigma Aldrich, USA). Ferric chloride hexahydrate ($FeCl_3 \cdot 6H_2O$, 12.5 mg) was then introduced to initiate polymerization, and the pH was adjusted to 0.8 using diluted hydrochloric acid. The reaction mixture was stirred for 1 h at room temperature to allow in situ formation of polypyrrole within the PVA/PEI matrix. In the PVA/PEI-PPY system, PVA functions as a structural scaffold/matrix, stabilizer, and soft template that improves the properties of conductive PPY composites. Its hydroxyl groups form hydrogen bonding interactions with PEI and PPY, promoting polymer alignment and controlled PPY growth. Additionally, PVA enhances mechanical flexibility, improves solution processability and viscosity, and prevents PPY aggregation, resulting in a more stable and uniformly dispersed composite system [31-34]. The resulting suspension was transferred into a dialysis membrane (MWCO 3.5 kDa) and dialyzed against deionized water for 3 days, with daily medium replacement, for removing unreacted species and by-products. The purified material was then lyophilized to obtain PVA/PEI-PPY composite powder. Photothermal performance was evaluated by dispersing PVA/PEI-PPY at various concentrations in deionized water, followed by sonication to obtain uniform suspensions. Samples were irradiated with an 808 nm NIR laser (2 W/cm^2) for 5 min, and temperature changes were recorded to assess time- and concentration-dependent photo thermal behavior. The selected NIR parameters were based on our previously established protocol and were maintained within a biologically safe range to avoid thermal damage while providing effective photo thermal stimulation [35,36].

2.1.2. Isolation and characterization of Tomato -derived extracellular vesicles

Fresh ripe Tomato were washed, destemmed, cut, and processed using a slow juicer to obtain juice, which was filtered to remove debris. The filtrate underwent differential centrifugation at 4 °C (3000 × g for 30 min, followed by 10,000 × g for 30 min, repeated twice) to remove larger particles as well as organelles. The supernatant was then filtered through a 0.22 μm membrane to obtain extracellular vesicles, which were aliquoted and stored at −80 °C. For nanoparticle tracking analysis (NTA), vesicles were diluted in PBS (10^7–10^{10} particles/mL), and particle size and concentration were measured based on Brownian motion using the instrument software.

2.1.3. ABTS radical scavenging assay

The antioxidant activity of Tomato -derived extracellular vesicles was evaluated using an ABTS radical scavenging assay. ABTS (7 mM, Abscience, Taiwan) and potassium persulfate (2.45 mM, Sigma Aldrich, Germany) were mixed (1:1) and incubated in the dark for 12 h to generate the radical solution. Vesicle suspensions at different concentrations were then added and incubated for 10 min, and absorbance was measured at 734 nm. Phosphate-buffered saline served as the negative control, and the scavenging rate was calculated accordingly. The equation is as follows

$$\text{Scavenging rate (\%)} = [(\text{A_control} - \text{A_sample}) / \text{A_control}] \times 100\%$$

2.1.4. Preparation, morphological and physicochemical and NIR-enhanced mechanical evaluation of TEV/PVA-PEI-PPY@GG hydrogel

TEV (1×10^{10} particles/mL) were combined with PVA/PEI-PPY dispersed in deionized water (1.5 mg/mL) and gellan gum solution (10 mg/mL, Thermofisher, Taiwan). After cooling the gellan gum below 40 °C, TEV were added and the mixture was stirred for 30 min to obtain a uniform composite hydrogel. For mechanical evaluation, the tested samples were exposed to 808 nm NIR irradiation (2 W/cm^2, 5 min), followed by compression testing using a texture analyzer for obtaining compressive strength. Hydrogel morphology was analyzed by SEM using freeze-dried, sputter-coated samples. Elemental composition was assessed by EDS, while FTIR (4000–500 cm^{-1}) identified functional groups and interactions. XRD (2θ = 10–80°) was used to evaluate crystallinity and structural integration.

2.1.5. In vivo diabetic wound model and histological evaluation

All animal experiments were approved with the Animal Ethics and Use Committee of Taipei Medical University (Approval No. SHLAC2025–0051) and conducted in accordance with institutional guidelines for animal care and use. Eight-week-old male Wistar rats (250–300 g) were used in this study. Diabetes was induced by intraperitoneal injection of streptozotocin (60 mg/kg), and only animals with blood glucose levels ≥ 250 mg/dL were included for further experiments. The sample size (n ≥ 3 per group) was selected based on studies and previous in vivo diabetic wound-healing reports to ensure reproducibility and statistical reliability. Animals were randomly assigned into experimental groups by means of a random allocation way. Animals that failed to meet the diabetic criteria or exhibited severe unrelated health complications were excluded prior to treatment allocation.

Under anesthesia, full-thickness excisional wounds (8 mm diameter) were created on the dorsal region of each animal, followed by topical administration of the respective treatments. Wound healing progression was monitored on days 1, 4, 8, and 12, and wound closure percentages were quantified using ImageJ software. Investigators involved in wound imaging, histological evaluation, and immunofluorescence quantification were blinded to the treatment groups during data collection and analysis to minimize observational bias. On day 12, animals were sacrificed and wound tissues were harvested for histological and immunofluorescence analyses. Hematoxylin and eosin (H&E) staining was performed to assess tissue regeneration, re-epithelialization, and dermal reconstruction. Quantitative analysis was performed using ImageJ software (National Institutes of Health, USA). Epidermal thickness was measured at five randomly selected locations within the wound area for each section and averaged to obtain a representative value. Inflammatory cell infiltration was evaluated using a semi-quantitative scoring system based on the density of inflammatory cells observed within the wound. Wound tissue sections were subjected to semi-quantitative histological assessment based on congestion, edema, hemorrhage, inflammatory cell infiltration, fibroblast proliferation, re-epithelialization, angiogenesis, and collagen deposition [37,38]. All measurements were performed on at least three non-overlapping fields per section by two independent investigators blinded to the treatment groups. The resulting values were averaged and expressed as mean ± standard deviation (SD) for statistical analysis. Immunofluorescence staining for AHR, TNF-α, CD31, and CD34 (all purchased from Bios Antibodies, USA) was further conducted to evaluate inflammatory response and angiogenic remodeling within the wound tissues.

2.2. Statistical analysis

Data are presented as mean ± standard deviation (SD). Statistical analyses were performed using GraphPad Prism software. Differences were considered statistically significant at $^*p < 0.05$, $^{**}p < 0.01$, and $^{***}p < 0.001$.

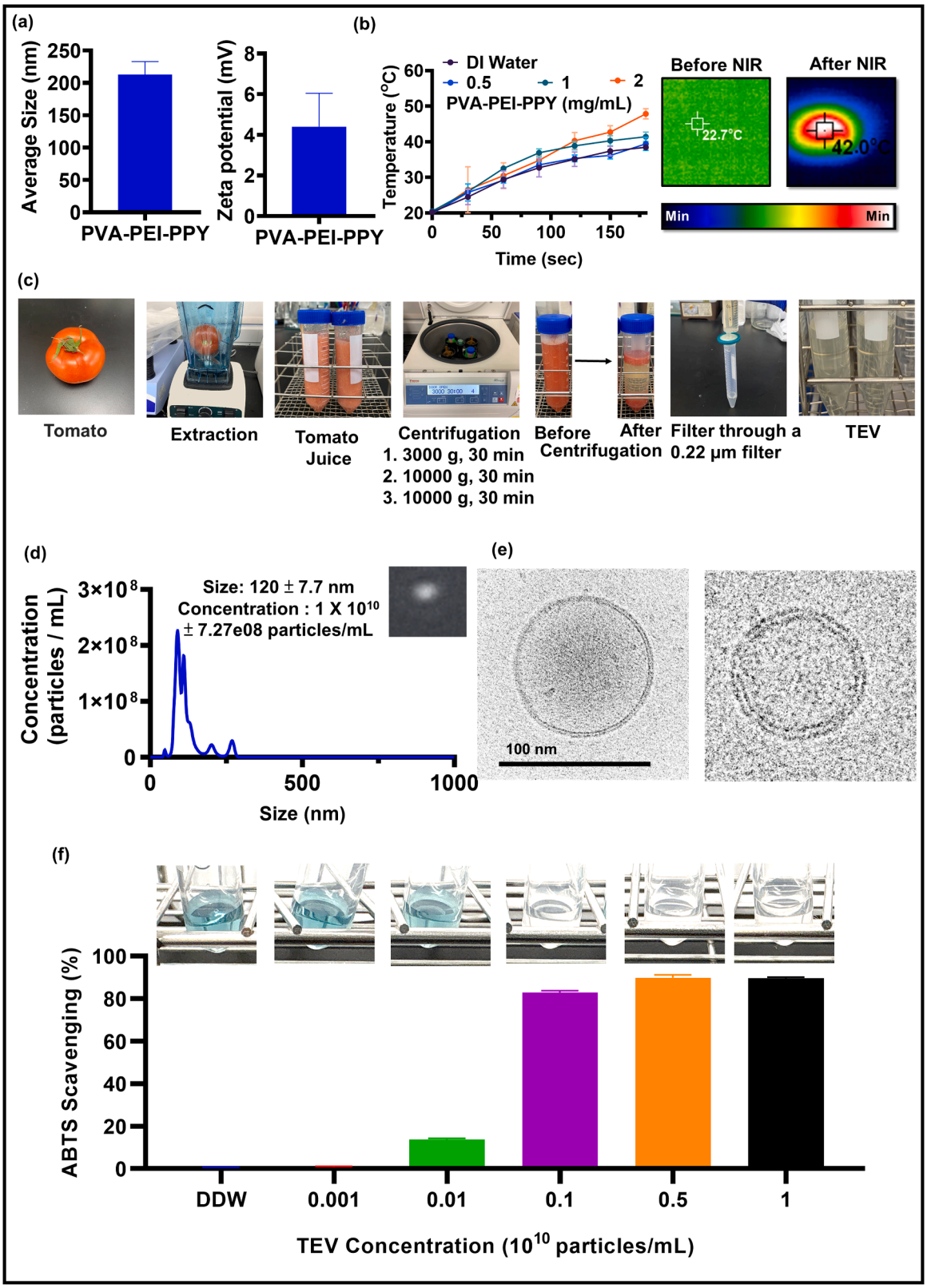

Fig. 1. Physicochemical characterization and functional evaluation of the Tomato EV-based platform. (a) Particle size and zeta potential (PVA-PEI-PPY). (b) Concentration-dependent photothermal profiles (PVA-PEI-PPY) under 808 nm NIR irradiation with thermal images. (c) Images of TEV extraction. (d) Nanoparticle tracking analysis showing size distribution (TEV). (e) Cryo-EM images of TEV showing characteristic spherical morphology and intact lipid bilayer membrane structures at the nanoscale. (f) ABTS assay demonstrating antioxidant activity of TEV.

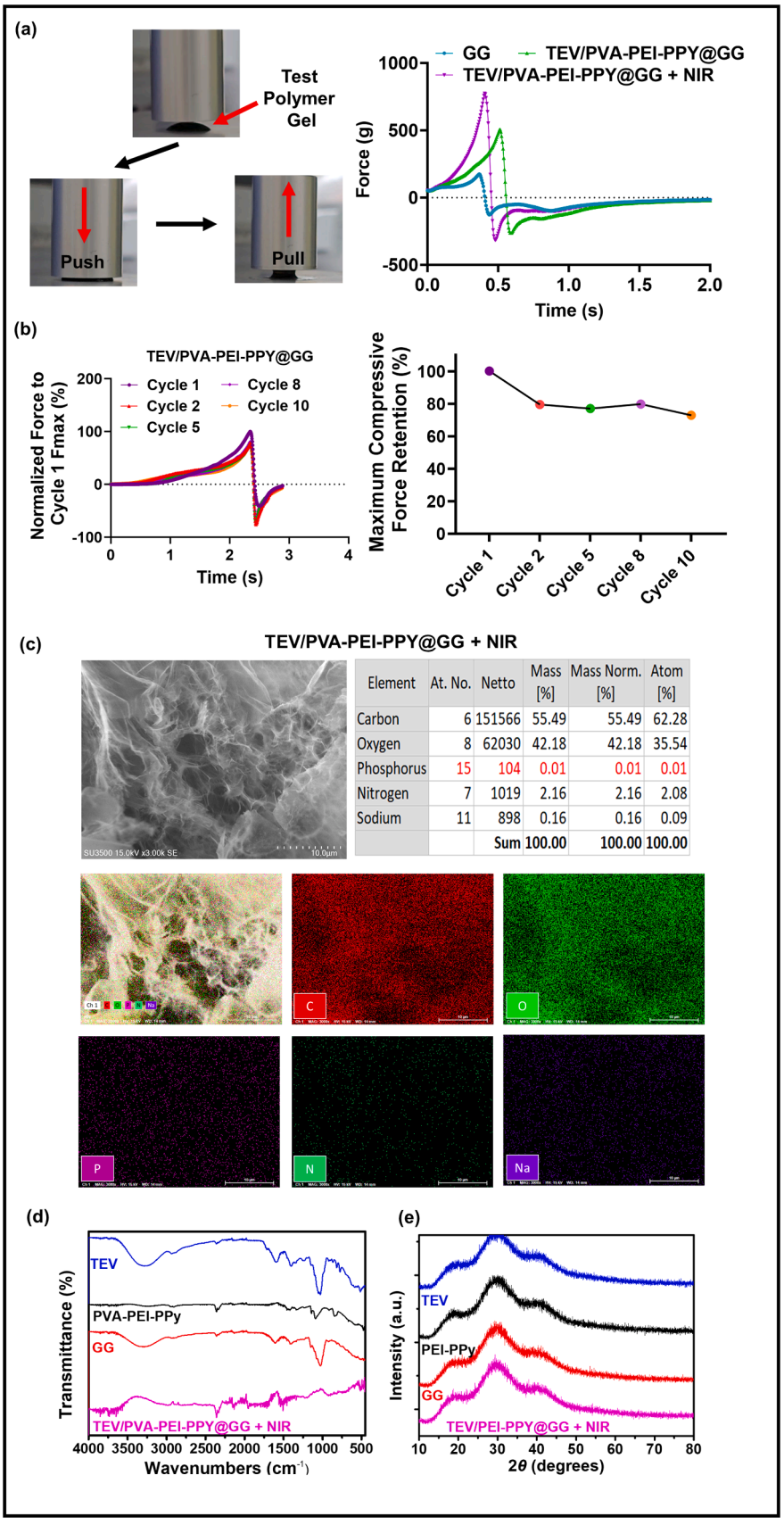

(caption on next page)

Fig. 2. Mechanical and structural characterization of the TEV/PVA-PEI-PPY@GG hydrogel. (a) Representative push–pull compression testing setup and corresponding force–time curves of GG, TEV/PVA-PEI-PPY@GG, and TEV/PVA-PEI-PPY@GG under NIR irradiation. (b) Cyclic compression performance as well as maximum compressive force retention of the TEV/PVA-PEI-PPY@GG hydrogel over repeated loading cycles, indicating enhanced mechanical stability and recovery behavior. (c) SEM image, elemental composition table, and EDS elemental mapping of the composite hydrogel. (d) FTIR spectra of formulations. (e) XRD patterns of formulations.

3. Results and discussion

3.1. Construction of a photothermally addressable and redox-active Tomato EV-based platform

Fig. 1**a** demonstrates that the nanosystem (PVA-PEI-PPY) exhibits a nanoscale size distribution with stable surface charge, indicating good colloidal stability. This supports uniform dispersion, effective carrier integration, and improved interaction with irregular diabetic wound surfaces, enhancing retention and therapeutic consistency [39-43]. Fig. 1**b** shows concentration-dependent photo thermal responsiveness under 808 nm NIR irradiation, with temperatures reaching mild hyperthermia (~42°C), confirming efficient light-to-heat conversion by the PPY-containing nanosystem [44-46]. Importantly, this mild hyperthermia promotes cellular activity, perfusion, and improves the wound microenvironment without causing thermal damage, while its tunability allows a balance between efficacy and safety [47-52]. TEV were isolated via homogenization, filtration, and differential centrifugation (Fig. 1**c**),

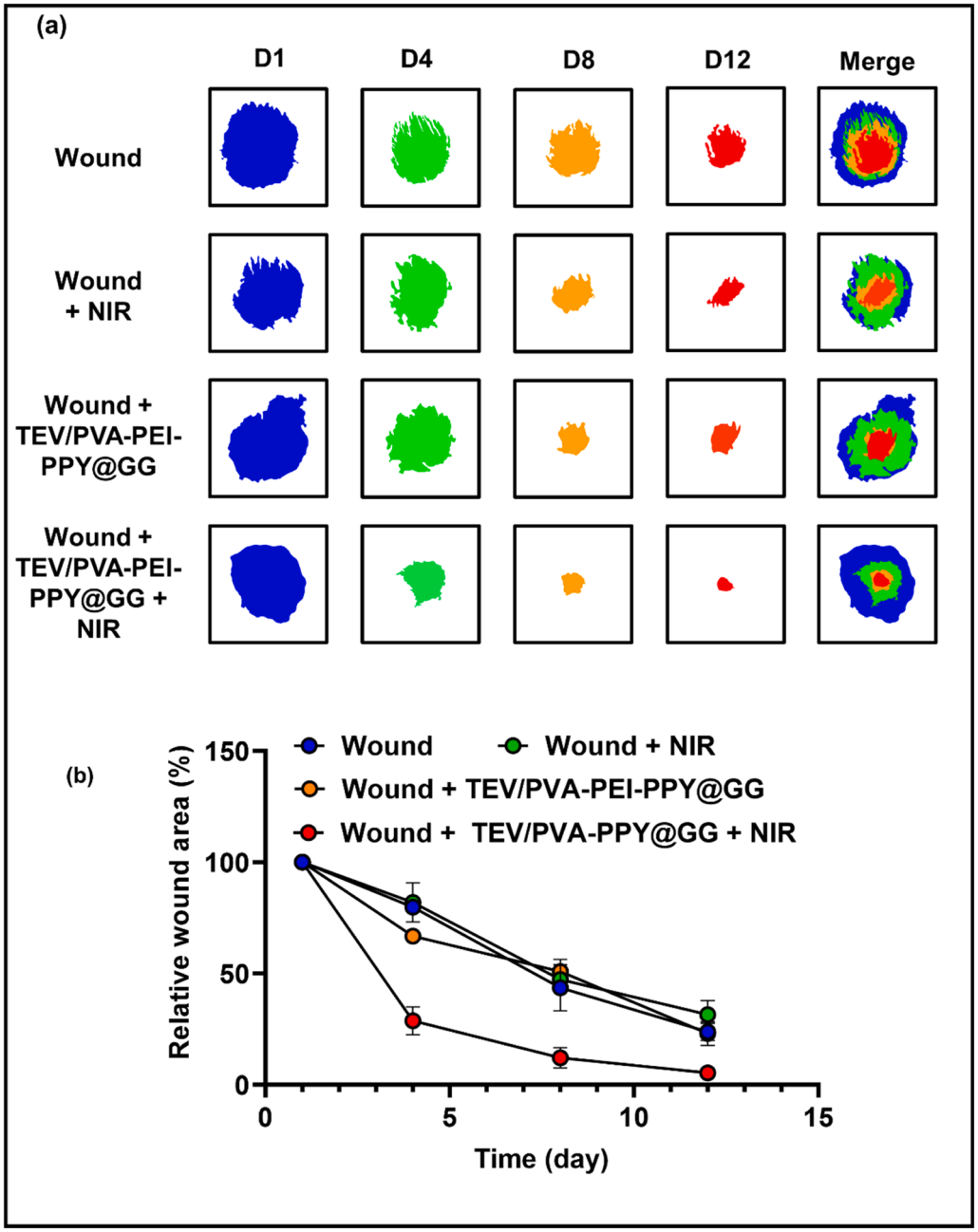

Fig. 3. In vivo evaluation of diabetic rats treated with the TEV/PVA-PEI-PPY@GG system. (a) Representative wound images and corresponding segmented areas over time processing using ImageJ. (b) Quantitative wound closure analysis. Data are presented as mean ± standard deviation (SD) (n ≥ 3 per group).

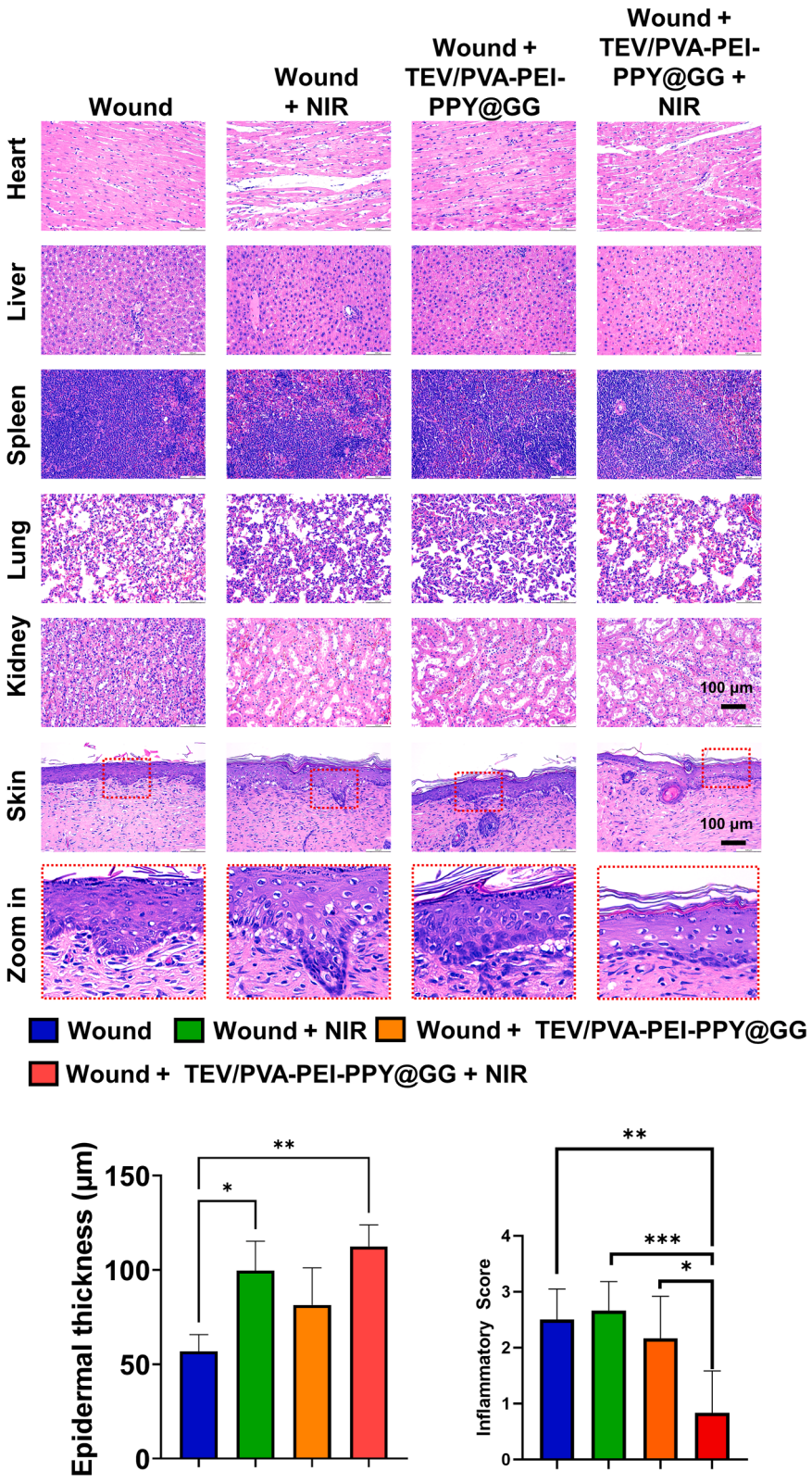

Fig. 4. Histological evaluation of major organs and wound tissues after treatment. Representative H&E-stained sections of the heart, liver, spleen, lung, and kidney showing systemic biosafety across groups, together with wound-skin sections and higher-magnification views illustrating re-epithelialization and tissue reconstruction after different treatments. Red dashed boxes indicate the enlarged regions. Quantitative analysis of epidermal thickness and inflammatory scoring among different treatment groups during wound healing. The wound + TEV/PVA-PEI-PPY@GG + NIR group exhibited the highest epidermal thickness and lowest inflammatory score, indicating enhanced re-epithelialization, reduced inflammation, and synergistic regenerative efficacy under combined hydrogel and NIR treatment. Data are presented as mean ± standard deviation (SD) ($n \geq 3$ per group). Statistical analyses were performed using GraphPad Prism. Differences were considered statistically significant at $^{*}p < 0.05$, $^{**}p < 0.01$, and $^{***}p < 0.001$.

with nanoparticle tracking analysis confirming nanoscale size (~130 nm) and a concentration of ~10^{10} particles/mL (Fig. 1**d**), suitable for material integration. Their small size supports efficient dispersion and bioactive interaction at the wound site. Cryo-electron microscopy (Cryo-EM) analysis indicated the isolation of TEV with a characteristic spherical morphology and clearly distinguishable lipid bilayer membrane structure (Fig. 1**e**). The vesicles exhibited nanoscale dimensions with intact membrane integrity as well as relatively uniform morphology, which are typical structural property of EVs. The preserved vesicular architecture observed under Cryo-EM further indicates the stability and purity of the isolated TEV without noticeable structural collapse or aggregation during sample preparation. ABTS assay results (Fig. 1**f**) demonstrated strong antioxidant activity, indicating effective redox-buffering capacity. Rich in bioactive compounds such as lycopene, TEV could reduce oxidative stress, promote M1-to-M2 macrophage polarization, and enhance skin cells (fibroblast and keratinocyte) bioactivity, accelerating wound healing. When incorporated into hydrogels, they offer a biocompatible and scalable approach for treating chronic wounds [14,53–55].

As shown in Fig. 2**a**, the hydrogel indicated stable and reversible responses under repeated compressive loading, reflecting its robust mechanical resilience. The compressive mechanical properties of the hydrogel were evaluated exploiting cyclic push-pull force analysis. The representative compression–decompression profiles validated that the TEV/PVA-PEI-PPY@GG hydrogel exhibited stable and reversible mechanical behavior under repeated loading cycles. Compared with the GG control, the incorporation of TEV/PEI-PPY enhanced the compressive force response, while NIR irradiation further improved the mechanical performance, indicating photo responsive reinforcement of the network of hydrogel. This performance likely arises from the interaction between the PPY framework and the GG matrix [56–58]. During cyclic testing (Fig. 2**b**), the hydrogel maintained consistent compressive force retention across multiple cycles, suggesting good elasticity, structural resilience, and preliminary cyclic compressive stability. Notably, the hydrogel retained a high percentage of its original compressive force after repeated deformation cycles, supporting the possibility of stable mechanical performance under repeated loading conditions. These findings indicate that the TEV/PVA-PEI-PPY@GG hydrogel possesses robust mechanical integrity suitable for biomedical and tissue engineering applications requiring repeated mechanical stress and deformation.

SEM analysis (Fig. 2**c**) indicated an interconnected porous fibrous structure that facilitates fluid exchange, exudate absorption, and sustained delivery of bioactive components. This architecture could support cell infiltration, nutrient and oxygen transport, and prevent hypoxia, so potentially promoting an optimal healing environment. The homogeneous, aggregation-free morphology also contributes to stable mechanical properties and supports multifunctional activities. EDS analysis confirmed uniform component distribution, with carbon and oxygen as major elements and nitrogen and phosphorus indicating the presence of PPY/PEI and TEV. FTIR results (Fig. 2**d**) revealed overlapping and shifted peaks, suggesting intermolecular interactions such as hydrogen bonding and electrostatic associations. Notably, changes after NIR treatment indicate that external stimulation can influence molecular or structure properties [59,60]. FTIR analysis confirmed successful integration of all components, with characteristic peaks retained in the composite. TEV showed C–H bending (~1470–1350 cm^{-1}) and C–O stretching (~1300–1000 cm^{-1}), along with bands at ~1230 and 1049 cm^{-1} (=C–H vibrations). PPY incorporation was indicated by the pyrrole ring peak at ~921 cm^{-1}. Gellan gum exhibited peaks at ~1620 cm^{-1} (C═O) and ~1030 cm^{-1} (C–O deformation). The preservation of these peaks without significant shifts confirms stable and unified incorporation of TEV, PPY, and GG in the composite system [61-65].

XRD analysis (Fig. 2**e**) showed broad diffraction patterns for both TEV and the composite, indicating a predominantly amorphous structure. 3D-printed personalized wound dressings represent a promising strategy for diabetic wound management, as they can be tailored for matching the exact geometry of irregular wounds using biocompatible hydrogel-based materials. Such customized dressings may provide improved wound coverage, reduced leakage and friction, controlled delivery of therapeutic agents, and optimized moisture regulation, so enhancing tissue regeneration and reducing infection risk. The adaptable and injectable nature of the developed hydrogel system may offer future potential for personalized and 3D-printable wound-healing applications, as per the reported literature [66-68].

3.2. In vivo wound-healing efficacy and functional improvement induced by the TEV/PVA-PEI-PPY@GG system

As shown in Fig. 3**a**, treated groups especially TEV/PVA-PEI-PPY@GG showed faster wound contraction and smaller residual areas compared to the experimental groups, indicating active tissue repair. Macroscopic wound processing using ImageJ software images (data) indicated gradual wound closure in all experimental groups over the 12-day treatment period. The untreated wound group showed delayed healing with a relatively larger residual wound area. Both NIR and TEV/PVA-PEI-PPY@GG treatments improved wound contraction compared with the wound-only group. Notably, the wound + TEV/PVA-PEI-PPY@GG + NIR group exhibited the greatest extent of wound closure and improved tissue regeneration among the experimental groups, suggesting enhanced wound healing outcomes under the combined treatment conditions. Quantitative analysis (Fig. 3**b**) confirmed higher closure rates, with the composite achieving the best performance. This effect likely results from combined hydrogel coverage, TEV antioxidant activity, and NIR-responsive PPY stimulation, addressing oxidative stress, inflammation, and impaired remodeling. The enhanced closure also suggests improved healing quality, including better re-epithelialization and granulation, indicating a shift from a chronic to a regenerative wound environment.

The findings suggest that the formulated material enhances both the speed and quality of wound healing compared to the other experimental groups. Treated wounds showed faster closure and more compact residual areas, reflecting active tissue regeneration rather than passive coverage, whereas control wounds exhibited delayed healing and larger unhealed regions typical of diabetic conditions [69-73]. Antioxidant compounds naturally present in ripe tomatoes may contribute to wound healing by reducing excessive oxidative stress and modulating prolonged inflammation during the healing process [74,75]. Tomatoes are rich in antioxidative constituents, including lycopene, β-carotene, ascorbic acid, vitamin E, vitamin C, and various phenolic compounds, which can help alleviate oxidative damage within the wound microenvironment and promote faster wound closure when incorporated into hydrogel systems [75]. So, both the TEV used in this study may contain these bioactive components, whose antioxidant properties could contribute to the observed enhancement in wound healing.

3.3. Histological and immunofluorescence evaluation confirms biosafety and enhanced regenerative response

H&E staining (Fig. 4) suggested good biosafety, with no abnormalities observed in major organs. The diabetic skin control group showed incomplete epidermis, thin neo-epithelium, and persistent inflammation, indicating impaired healing, whereas treated groups especially TEV/PVA-PEI-PPY@GG seems a thicker, continuous epidermis with potentially improved keratinization, reflecting enhanced re-epithelialization and barrier restoration [76-80]. Quantitative analysis of epidermal thickness revealed possible differences among the treatment groups. The wound-only group showed an epidermal thickness of 56.8933 μm, indicating limited epidermal regeneration. The wound + NIR group exhibited a markedly increased epidermal thickness of 99.6989 μm, supporting the possibility that NIR stimulation contributed to epidermal remodeling.

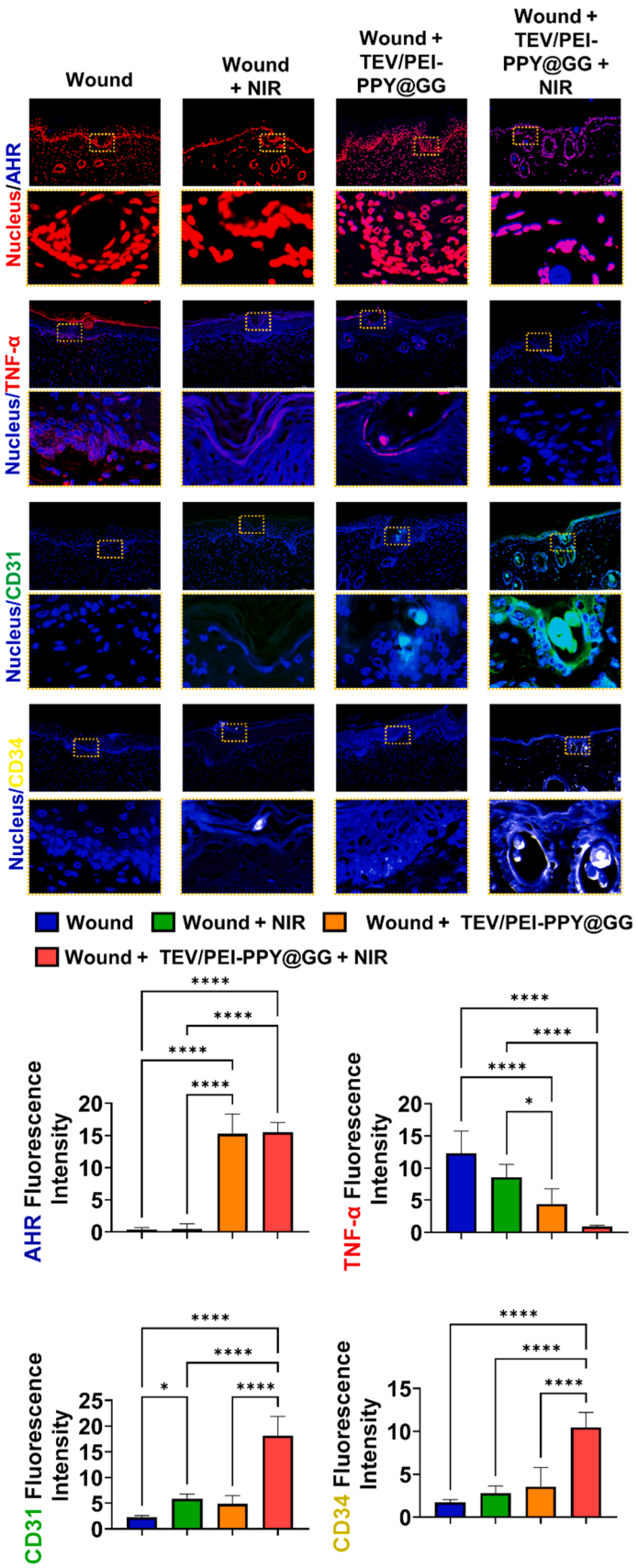

Fig. 5. Immunofluorescence staining of wound tissues for AHR, TNF-α, CD31, and CD34 after different treatments. Representative fluorescence images and corresponding enlarged views are shown, together with quantitative analysis of marker expression. Nuclei were counterstained with DAPI or PI. Yellow dashed boxes indicate the enlarged regions. Data are presented as mean ± standard deviation (SD) ($n \geq 3$ per group). Statistical analyses were performed using GraphPad Prism. Differences were considered statistically significant at $^{*}p < 0.05$, $^{**}p < 0.01$, and $^{***}p < 0.001$.

Treatment with TEV/PVA-PEI-PPY@GG causes an epidermal thickness of 81.4718 μm, demonstrating moderate improvement in tissue regeneration. Notably, the wound + TEV/PVA-PEI-PPY@GG + NIR group displayed the highest epidermal thickness (112.474 μm), indicating significantly enhanced re-epithelialization and skin tissue regeneration under combined hydrogel and NIR treatment. These findings suggest a synergistic regenerative effect of TEV/PVA-PEI-PPY@GG and NIR irradiation in promoting epidermal restoration during wound healing. Histopathological inflammatory scoring revealed that the wound and wound + NIR groups exhibited relatively high inflammatory responses, indicating persistent inflammation at the wound site. Treatment with TEV/PVA-PEI-PPY@GG alone moderately reduced the inflammatory score, which may contribute to an improved inflammatory microenvironment. Notably, the wound + TEV/PVA-PEI-PPY@GG + NIR group suggest the lowest inflammatory score among all groups, indicating significant suppression of inflammatory cell infiltration and enhanced resolution of inflammation. Statistical analysis confirmed significant differences between the treatment groups, highlighting the synergistic anti-inflammatory effect of TEV/PVA-PEI-PPY@GG under NIR irradiation.

Immunofluorescence analysis (Fig. 5) further showed increased AHR expression in the treated groups, particularly in the TEV/PVA-PEI-PPY@GG group, which may contribute to the establishment of a regenerative microenvironment. This effect is likely driven by PPY-mediated NIR photo thermal stimulation, which reduces oxidative stress as well as promotes repair via AHR signaling, highlighting the combined photo thermal and immunomodulatory benefits of the system [81-83].

TNF-α showed the opposite trend to AHR, with high expression in the diabetic control but markedly lower levels in the treated groups, indicating effective suppression of inflammation. This likely attributed to the combined antioxidant activity of TEV and the mild NIR-induced photothermal effect of PPY, which together improved the wound microenvironment. The inverse AHR/TNF-α pattern further suggests a shift from chronic inflammation toward a repair-supportive healing state [84-88]. CD31 and CD34 were markedly increased in the treated groups, especially in the TEV/PVA-PEI-PPY@GG group, indicating enhanced angiogenesis versus the other groups. This suggests improved oxygen and nutrient delivery to the wound site. Overall, Fig. 5 shows that the platform promotes a regenerative microenvironment by enhancing AHR signaling, suppressing TNF-α–mediated inflammation, and stimulating vascular formation through its combined photothermal and antioxidant effects.

4. Conclusion

Lastly, a multifunctional TEV/PVA-PEI-PPY@GG hydrogel dressing was formulated for diabetic wound healing by integrating TEV, a conductive PPY-based NIR-responsive component, and a biocompatible gellan gum hydrogel matrix. The prepared hydrogel platform indicated favorable physicochemical characteristics, including structural stability, hydrogel integration, antioxidant activity, and mild photothermal responsiveness under NIR irradiation, supporting its suitability as a bioactive wound dressing system. In the diabetic wound model, the hydrogel promoted wound closure and improved tissue regeneration, as supported by histological analysis. In addition, no obvious histopathological abnormalities were observed in major organs, indicating acceptable in vivo biocompatibility under the applied treatment conditions. Immunofluorescence staining revealed altered expression patterns of AHR, TNF-α, CD31, and CD34 in treated tissues, which were associated with improved wound healing outcomes and may contribute to tissue repair processes. These observations support the possibility that the hydrogel creates a favorable local environment for wound regeneration. Collectively, these findings indicate that the TEV/PVA-PEI-PPY@GG hydrogel combines bioactive supported by externally responsive photothermal properties and is associated with enhanced wound healing performance. While further studies are required to elucidate the underlying molecular pathways and biological interactions, the present findings support the potential of plant EV-integrated multifunctional hydrogels as a therapeutic approach for diabetic wound healing and tissue regeneration.

Author contributions

All authors have approved the final version of the manuscript.

CRediT authorship contribution statement

Yao-Jen Chang: Methodology, Investigation, Data curation, Formal analysis, Writing – original draft. **Yao-Wei Liou:** Methodology, Investigation, Data curation, Formal analysis, Writing – original draft. **Lekshmi Rethi:** Investigation, Data curation, Formal analysis, Writing – original draft. **Sih-Chi Chuang:** Writing – review & editing. **Pei-Chia Hung:** Writing – review & editing. **Ching-Cheng Huang:** Writing – review & editing. **Yi-Ting Shu:** Conceptualization, Investigation, Writing – review & editing. **Jie-Fan Chang:** Conceptualization, Investigation, Writing – review & editing. **Chiou-Shann Fuh:** Conceptualization, Investigation, Writing – review & editing. **Andrew E.-Y. Chuang:** Conceptualization, Supervision, Investigation, Funding acquisition, Project administration, Writing – review & editing.

Consent for publication

All of the authors involved in this study have agreed to its publication.

Ethics approval and consent to participate

This study was approved under the guidelines of the Animal Ethics and Use Committee of Taipei Medical University.

Declaration of Competing Interest

The authors declare that they have no known competing financial interests or personal relationships that could have appeared to influence the work reported in this paper.

Acknowledgments

This work was supported by the National Science and Technology Council (NSTC), Taiwan [114–2628-E−038–001-MY3], the National Health Research Institutes (NHRI) of Taiwan (NHRI-EX115–11323EI), and Taipei Medical University–Shin Kong Wu Ho-Su Memorial Hospital (SKH-TMU−115–02). The authors also acknowledge the use of Grammarly, ChatGPT, and BioRender for language refinement/editing and figure preparation.

Data availability

Data will be made available on request.

References

[1] R. Wang, S. Gu, Y.H. Kim, A. Lee, H. Lin, D. Jiang, Diabetic Wound Repair: From Mechanism to Therapeutic Opportunities, MedComm (2020) 6 (2025) e70406.
[2] N. Dasari, A. Jiang, A. Skochdopole, J. Chung, E.M. Reece, J. Vorstenbosch, S. Winocour, Updates in Diabetic Wound Healing, Inflammation, and Scarring, Semin. Plast. Surg. 35 (2021) 153–158.
[3] L. Deng, C. Du, P. Song, T. Chen, S. Rui, D.G. Armstrong, W. Deng, The Role of Oxidative Stress and Antioxidants in Diabetic Wound Healing, Oxid. Med. Cell. Longev. 2021 (2021) 8852759.
[4] T.M. Bauer, J.Y. Moon, J. Shadiow, S.D. Buckley, K.A. Gallagher, Mechanisms of Impaired Wound Healing in Type 2 Diabetes: The Role of Epigenetic Factors, Arterioscler. Thromb. Vasc. Biol. 45 (2025) 632–642.

[5] J. Song, T. Zhao, C. Wang, X. Sun, J. Sun, Z. Zhang, Cell migration in diabetic wound healing: Molecular mechanisms and therapeutic strategies (Review), Int. J. Mol. Med. 56 (2025) 126.
[6] Y. Hu, D. Xv, C. Xie, X. Lu, Smart self-healing hydrogel wound dressings for diabetic wound treatment, Nanomed. (Lond.) 20 (2025) 737–754.
[7] H. Wang, L.-M. Zhang, Intelligent biobased hydrogels for diabetic wound healing: A review, Chem. Eng. J. 484 (2024) 149493.
[8] B. Bhattacharjee, S. K, D. Rynjah, P. Kalita, A. Newar, K. Kalita, S. Sarma, P. P. Dutta, M.J. Kapil, A.B. Ahmed, R.K. Sahu, Recent trends in hydrogel-based formulation for the treatment of diabetic wounds: a review, J. Drug. Deliv. Sci. Tec. 107 (2025) 106848.
[9] J. He, J. Chen, T. Liu, F. Qin, W. Wei, Research progress of multifunctional hydrogels in promoting wound healing of diabetes, Int. J. Nanomed. 20 (2025) 7549–7578.
[10] X. He, Y. Wei, K. Xu, Hydrogel-based treatment of diabetic wounds: from smart responsive to smart monitoring, Gels 11 (2025) 647.
[11] M.Q. Lian, W.H. Chng, J. Liang, H.Q. Yeo, C.K. Lee, M. Belaid, M. Tollemeto, M. G. Wacker, B. Czarny, G. Pastorin, Plant-derived extracellular vesicles: recent advancements and current challenges on their use for biomedical applications, J. Extracell. Vesicles 11 (2022) e12283.
[12] D. Primorac, P. Brlek, L. Bulić, N. Hrvatin, V. Škaro, P. Projić, M. Glavan, I. Oleru, P. Rocheteau, C. Tremolada, A. DeMers, M.A. Ambach, D. Buford, T. Knežević, D. Kouroupis, C. Conforti, D.W. Kimbrough, R.P. Schnorr, L. Williams, R. Vaiciuleviciute, Ž. Fortuna, L. Opršnik, B. Curk, M. Knežević, G. Kalan Živčec, A. Hrkać, D. Tsoukas, I. Uzieliene, J. Pachaleva, E. Bernotiene, K. Barbato, N. Patel, I.D. Guanche, E.V. Badiavas, J. Mešić, A. Medić Flajšman, R. Milanič, D. Klarić, V. E. Kalodimou, M. Allegri, J. Brachmann, W.S. Toh, N.D. Delgado, A. Mobasheri, Therapeutic potential of extracellular vesicles: from biogenesis, isolation and molecular characterization to addressing translational gaps and regulatory barriers, Int. J. Mol. Sci. 27 (2026) 1676.
[13] X. Guan, M. Zhu, H. Zhu, Q. Wang, J. Chen, Y. Chen, X. Mou, J. Si, Oral natural extracellular vesicles for biomedical applications: Advances and clinical perspectives, J. Adv. Res. 83 (2025) 1105–1125.
[14] V. Daniello, V. De Leo, M. Lasalvia, M.N. Hossain, A. Carbone, L. Catucci, R. Zefferino, C. Ingrosso, M. Conese, S. Gioia, Solanum lycopersicum (Tomato)-Derived Nanovesicles Accelerate Wound Healing by Eliciting the Migration of Keratinocytes and Fibroblasts, Int. J. Mol. Sci. 25 (2024) 2452.
[15] K. Włodarczyk, B. Smolińska, I. Majak, The Antioxidant Potential of Tomato Plants (Solanum lycopersicum L.) under Nano-ZnO Treatment, Int. J. Mol. Sci. 24 (2023) 11833.
[16] S. Wang, F. Wang, X. Zhao, F. Yang, Y. Xu, F. Yan, D. Xia, Y. Liu, The effect of near-infrared light-assisted photothermal therapy combined with polymer materials on promoting bone regeneration: A systematic review, Mater. & Des. 217 (2022) 110621.
[17] Y. Wang, R. Garg, D. Cohen-Karni, T. Cohen-Karni, Neural modulation with photothermally active nanomaterials, Nat. Rev. Bioeng. 1 (2023) 193–207.
[18] X. Kong, X. Zhang, Y. Wang, B. Zhang, Recent Advances of Photothermal Materials for Biomedical Applications, ACS Omega 10 (2025) 38345–38358.
[19] C. chih-wei, A.E.Y. Chuang, Biofunctional core-shell polypyrrole–polyethylenimine nanocomplex for a locally sustained photothermal with reactive oxygen species enhanced therapeutic effect against lung cancer, Int. J. Nanomed. 14 (2019) 1575–1585.
[20] Z. Chu, X. Liu, T. Zhao, D. Jiang, J. Zhao, X. Dong, K.W.K. Yeung, X. Liu, Y. Liao, L. Ouyang, Self-healing Ppy-hydrogel promotes diabetic skin wound healing through enhanced sterilization and macrophage orchestration triggered by NIR, Biomaterials 315 (2025) 122964.
[21] S. Deng, X. Huang, Z. Kang, D. Xu, W. Luo, D. Li, Adoption of polyvinyl alcohol electrospinning materials for skin wound dressing, J. Mater. Sci. Mater. Med. 36 (2025) 84.
[22] Y.C. Hsiao, P.R. Jheng, H.T. Nguyen, Y.H. Chen, Y.B. Manga, L.S. Lu, L. Rethi, C. H. Chen, T.W. Huang, J.D. Lin, T.K. Chang, Y.C. Ho, E.Y. Chuang, Photothermal-Irradiated Polyethyleneimine-Polypyrrole Nanopigment Film-Coated Polyethylene Fabrics for Infrared-Inspired with Pathogenic Evaluation, ACS Appl. Mater. Interfaces 13 (2021) 2483–2495.
[23] M. Li, Y. Han, B. Cai, Y. Jiang, B. Zhang, F. Yuan, C. Zhou, Cao, Muscle-inspired MXene/PVA hydrogel with high toughness and photothermal therapy for promoting bacteria-infected wound healing, Biomater. Sci. -Uk Y (2022) 1068–1082.
[24] Y.-C. Hsiao, P.-R. Jheng, H.T. Nguyen, Y.-H. Chen, Y.B. Manga, L.-S. Lu, L. Rethi, C.-H. Chen, T.-W. Huang, J.-D. Lin, T.-K. Chang, Y.-C. Ho, E.-Y. Chuang, Photothermal-Irradiated Polyethyleneimine–Polypyrrole Nanopigment Film-Coated Polyethylene Fabrics for Infrared-Inspired with Pathogenic Evaluation, ACS Appl. Mater. & Interfaces 13 (2021) 2483–2495.
[25] E.D. Quiñones, T.-Y. Lu, K.-T. Liu, Y.-J. Fan, E.-Y. Chuang, J. Yu, Glycol chitosan/iron oxide/polypyrrole nanoclusters for precise chemodynamic/photothermal synergistic therapy, Int. J. Biol. Macromol. 203 (2022) 268–279.
[26] Z. Feketshane, S. Alven, B.A. Aderibigbe, Gellan Gum in Wound Dressing Scaffolds, Polym. (Basel) 14 (2022) 4098.
[27] F. Lalebeigi, A. Alimohamadi, S. Afarin, H.Aghamirza Moghim Aliabadi, M. Mahdavi, F. Farahbakhshpour, N. Hashemiaval, K. Khandari, R. eivazzadeh-keihan, A. Maleki, Recent advances on biomedical applications of gellan gum: A review, Carbohyd Polym. 334 (2024) 122008.
[28] A. Saleem, I.U. Khan, Y. Kamal, Y. Mehmood, Z. Chauhdary, M. Irfan, S.H. Khalid, H.U. Khan, Usra, G. Hussain, A. Bouallegue, A.A. Mengistie, R.N. Herqash, E. M. Alyami, A.R. Alanzi, Gellan gum-based composites hydrogel membranes with geranium and lemongrass oils for enhanced antibacterial and wound healing effect, Sci. Rep. 15 (2025) 39179.
[29] L. Yuan, X. Jiang, M. Jiang, Y. Guo, Y. Liu, P. Ming, S. Li, P. Zhou, R. Cai, K. Yu, G. Tao, Biocompatible gellan gum/sericin hydrogels containing halloysite@polydopamine nanotubes with hemostasis and photothermal antibacterial properties for promoting infectious wound repair, Mater. & Des. 227 (2023) 111744.
[30] A. Ansari, M.S. Shaikh, M.U.M. Siddique, M. Khairnar, S.S. Ali, S.N. Goyal, M. S. Hasnain, A. Bose, A.K. Nayak, Chapter 12 - Gellan gum–based wound dressings, in: A.K. Nayak, M.S. Hasnain (Eds.), Application of Gellan Gum as a Biomedical Polymer, Academic Press, 2024, pp. 251–264.
[31] N.R. Karakuş, S. Türk, G. Guney Eskiler, M. Syzdykbayev, N.O. Appazov, M. Özacar, Investigation of Tannic Acid Crosslinked PVA/PEI-Based Hydrogels as Potential Wound Dressings with Self-Healing and High Antibacterial Properties, Gels 10 (2024) 682.
[32] L. Shao, J. Li, Y. Guang, Y. Zhang, H. Zhang, X. Che, Y. Wang, PVA/polyethyleneimine-functionalized graphene composites with optimized properties, Mater. & Des. 99 (2016) 235–242.
[33] C. Dong, X. Yuan, M. He, Preparation of PVA/PEI ultra-fine fibers and their composite membrane with PLA by electrospinning, J. Biomater. Sci. Polym. Ed. 17 (2006) 631–643.
[34] H.P. de Oliveira, M.V.B. dos Santos, C.G. dos Santos, C.P. de Melo, Preparation and electrical and dielectric characterization of PVA/PPY blends, Mater. Charact. 50 (2003) 223–226.
[35] D. Báez, Graphene-Based Nanomaterials for Photothermal Therapy in Cancer Treatment, Pharmaceutics 15 (2023) 2286.
[36] Q. Ding, J. Liu, Y. Wang, J. Kim, Z. Huang, Y. Lee, H. Zhou, P. Zhang, J.L. Sessler, J. S. Kim, Dual-laser "808 and 1,064 nm" strategy that circumvents the Achilles' heel of photothermal therapy, Proc. Natl. Acad. Sci. USA 122 (2025) e2503574122.
[37] M.A. Abu-Al-Basal, Healing potential of Rosmarinus officinalis L. on full-thickness excision cutaneous wounds in alloxan-induced-diabetic BALB/c mice, J. Ethnopharmacol. 131 (2010) 443–450.
[38] A.A. Khalaf, E.I. Hassanen, A.R. Zaki, A.F. Tohamy, M.A. Ibrahim, Histopathological, immunohistochemical, and molecular studies for determination of wound age and vitality in rats, Int. Wound J. 16 (2019) 1416–1425.
[39] J. Nandhini, E. Karthikeyan, S. Rajeshkumar, Nanomaterials for wound healing: Current status and futuristic frontier, Biomed. Technol. 6 (2024) 26–45.
[40] P. Paul, S.S. Hakkimane, Nanoparticle-based approaches for wound healing: a comprehensive review of nanomaterials enhancing tissue regeneration, Discov. Nano 20 (2025) 201.
[41] N. Vodolazkaya, A. Laguta, V. Farafonov, M. Nikolskaya, Z. Balklava, R. Khayat, M. Stich, N. McHedlov-Petrossyan, D. Nerukh, Influence of various colloidal surfactants on the stability of MS2 bacteriophage suspension. The charge distribution on the PCV2 virus surface, J. Mol. Liq. 387 (2023) 122644.
[42] A. Aliyev, A. Israyilova, U. Hasanova, Z. Gakhramanova, A. Ahmadova, Nanotechnology in Wound Healing: A New Frontier in Regenerative Medicine, Micro 5 (2025) 60.
[43] L. Guerrini, R.A. Alvarez-Puebla, N. Pazos-Perez, Surface Modifications of Nanoparticles for Stability in Biological Fluids, Mater. (Basel) 11 (2018) 1154.
[44] Z. Xiong, H. Zhang, Y. Zhou, Y. Yang, Preparation of PCU/PPy composites with self-healing and UV shielding properties, Front. Mater. 9 (2022) 2022.
[45] Y. Sood, S.D. Lawaniya, H. Mudila, K. Awasthi, A. Kumar, Polypyrrole-Tungsten disulphide 2D nanocomposites for ammonia sensing, Sens. Actuators B Chem. 394 (2023) 134298.
[46] T. Zhang, J. Zhai, Z. Shi, Q. Li, J. Cai, Comparison of PV and PV/T systems in different regions of China: Energy gain, energy cost, energy payback and energy return, Energy Built Environ. 7 (2026) 253–266.
[47] M. Amin, W. Huang, A.L.B. Seynhaeve, T.L.M. Ten Hagen, Hyperthermia and Temperature-Sensitive Nanomaterials for Spatiotemporal Drug Delivery to Solid Tumors, Pharmaceutics 12 (2020) 1007.
[48] S. Kumar, P. Nasna, G. Ghosh, Recent advancement in biocompatible materials, hybrid bioactive coating, surface modification and post-processing techniques for the fabrication of biomedical implant: Critical review and future prospects, Proceedings Institution Mechanical Engineers Part C Journal Mechanical Engineering Science 239 (2025) 3247–3286.
[49] D. Gazel, H. Demirbakan, M. Erinmez, In vitro activity of hyperthermia on swarming motility and antimicrobial susceptibility profiles of Proteus mirabilis isolates, Int. J. Hyperth. 38 (2021) 1002–1012.
[50] Z. Yu, W.K. Chan, Y. Zhang, T.T.Y. Tan, Near-infrared-II activated inorganic photothermal nanomedicines, Biomaterials 269 (2021) 120459.
[51] Z. Bei, L. Ye, Q. Tong, Y. Ming, T. Yang, Y. Zhu, L. Zhang, X. Li, H. Deng, J. Liu, W. Chen, B. Chu, Z. Qian, Thermostimulated shrinking and adhesive hydrogel dressing for treating chronic diabetic wounds, Cell. Rep. Phys. Sci. 5 (2024) 102289.
[52] P. Harder, N. İyisan, C. Wang, F. Kohler, I. Neb, H. Lahm, M. Dreßen, M. Krane, H. Dietz, B. Özkale, A Laser-Driven Microrobot for Thermal Stimulation of Single Cells, Adv. Healthc. Mater. 12 (2023) 2300904.
[53] V. Daniello, V. De Leo, M. Lasalvia, M.N. Hossain, A. Carbone, L. Catucci, R. Zefferino, C. Ingrosso, M. Conese, S. Di Gioia, Solanum lycopersicum (Tomato)-Derived Nanovesicles Accelerate Wound Healing by Eliciting the Migration of Keratinocytes and Fibroblasts, Int. J. Mol. Sci. 25 (2024) 2452.
[54] B. Zhang, L. Yu, L. Tang, Methacrylamide Hyaluronic Acid/Tannic Acid Hydrogel Loaded with Tomato and HEK 293 Cell-Derived Exosomes for Diabetic Wound Repair, ACS Biomater. Sci. & Eng. 12 (2026) 1106–1126.

[55] X. Jianda, Y. Zimo, D. Yuhan, X. Zhongyu, Z. Kewei, C. Xiaolan, Plant-derived extracellular vesicles in diabetic wound healing: mechanisms, therapeutic implications and future perspectives, J. Mater. Sci. Mater. Med. 36 (2025) 107.
[56] M. Zhang, Y. Zhang, J. Sun, W. Feng, R. Li, Physically crosslinked, montmorillonite-reinforced hydrogels for self-healing and tough adhesive wound dressings, J. Mater. Sci. 61 (2026) 526–542.
[57] Y. Deng, P. Li, X. Peng, S. Feng, X. Yu, Q. Zhao, Quaternary ammonium chitosan/N-isopropylacrylamide-based Janus hydrogel with asymmetric adhesive, shrinkable, and antimicrobial properties for wound healing, Int. J. Biol. Macromol. 327 (2025) 147416.
[58] Q. Hu, Y. Du, Y. Bai, D. Xing, S. Lang, K. Li, X. Li, Y. Nie, G. Liu, Sprayable Zwitterionic Antibacterial Hydrogel With High Mechanical Resilience and Robust Adhesion for Joint Wound Treatment, Macromol. Rapid Commun. 45 (2024) 2300683.
[59] K. Huang, W. Liu, W. Wei, Y. Zhao, P. Zhuang, X. Wang, Y. Wang, Y. Hu, H. Dai, Photothermal Hydrogel Encapsulating Intelligently Bacteria-Capturing Bio-MOF for Infectious Wound Healing, Acs Nano 16 (2022) 19491–19508.
[60] J. Guo, W. Lei, B. Li, K. Li, J. Li, Z. Wang, H. Liu, C. Huang, Y. Shen, Injectable living hydrogel as engineered biotherapeutic to promote tooth-extraction wound healing and alveolar bone regeneration, Bioact. Mater. 59 (2026) 355–369.
[61] O. Comfort, I. Ochida, B. Adams, A. Anhwange, N. Nwanganga, Abah, Chemical and microbial quality evaluation of fresh tomato and its processed products using FTIR, SEM GC-MS 07 (2019) 30–44.
[62] R. Saberi Riseh, M. Moradipour, A novel encapsulation of Streptomyces fulvissimus Uts22 by spray drying and its biocontrol efficiency against Gaeumannomyces graminis, the causal agent of take-all disease in wheat, Pest. Manag. Sci. 77 (2021) 4357–4364.
[63] Z. Ahmad, M.Aziz Choudhary, A. Mehmood, R. Wakeel, T. Akhtar, M. Rafiq, Synthesis of polypyrrole nano/microspheres using cobalt(III) as an oxidizing agent and its ammonia sensing behavior, Macromol. Res. 24 (2016).
[64] M.T. Ramesan, Synthesis, characterization, and conductivity studies of polypyrrole/copper sulfide nanocomposites, J. Appl. Polym. Sci. 128 (2013) 1540–1546.
[65] Y. Fu, A. Manthiram, Sulfur-Polypyrrole Composite Cathodes for Lithium-Sulfur Batteries, RSC Adv. 2 (2012) 5927–5929.
[66] R. Kabra, N. Poonia, R.N. Subudhi, T. Singh, G. Joshi, R. Sharma, V. Arora, Innovative strategies for the management of diabetic wounds: A step toward faster recovery, J. Drug. Deliv. Sci. Tec. 115 (2026) 107824.
[67] M. Farhadi, S. Moghari, M. Naqvi, H.A. Khonakdar, Recent Advances in Biodegradable Polymers for Wound Dressings, Infection, and Diabetes Treatment: A Review, Polym. Eng. & Sci. 65 (2025) 6377–6408.
[68] N. Kim, H. Lee, G. Han, M. Kang, S. Park, D.E. Kim, M. Lee, M.J. Kim, Y. Na, S. Oh, S.J. Bang, T.S. Jang, H.E. Kim, J. Park, S.R. Shin, H.D. Jung, 3D-Printed Functional Hydrogel by DNA-Induced Biomineralization for Accelerated Diabetic Wound Healing, Adv. Sci. (Weinh.) 10 (2023) e2300816.
[69] C. Makwana, V.P. Mehta, S. Singh, M. Suvariya, A Comparative Study of Regular Dressing versus Negative Dressing in Management of Patients with Diabetic Foot, Adv. Human. Biol. 14 (2024) 68–72.
[70] MolecuLight, 2020, Document the Path of Wound Healing with MoleuLight i: XMolecuLight Webpage.
[71] D. Lou, Q. Pang, X. Pei, S. Dong, S. Li, W.-q. Tan, L. Ma, Flexible wound healing system for pro-regeneration, temperature monitoring and infection early warning, Biosens. Bioelectron. 162 (2020) 112275.
[72] N.S. Mondal, A. Islam, M.K. Gautam, S. Mondal, M. Ahmed, S. Jamir, L. D. Khongwir, B. Mahajon, Unraveling the Mechanisms of Diabetic Wounds: Insights into Pathogenesis and Advanced Treatment Strategies, Curr. Diabetes Rev. 22 (2026) 113–136.
[73] K. Karnam, K. Sedmaki, P. Sharma, V.V.K. Venuganti, O.P. Kulkarni, Selective inhibition of PKR by C16 accelerates diabetic wound healing by inhibiting NALP3 expression in mice, Inflamm. Res. 72 (2023) 221–236.
[74] E.E.-E. Innocent, P.C. Wokpeogu, W.B. Sudor, P.J. Nwolim, The effect of ethanolic seed extract of Solanum lycopersicum on wound healing, Eur. J. Pharm. Med. Res. 5 (2017) 356–361.
[75] Y. Fang, G. Li, C. Huang, K. Huang, Y. Zhao, T. Nie, J. Wu, Tomato based gelatin methacryloyl hydrogel as an effective natural and low-cost scaffold for accelerative wound healing, Int. J. Biol. Macromol. 229 (2023) 123–135.
[76] X.T. Wang, C.C. McKeever, P. Vonu, C. Patterson, P.Y. Liu, Dynamic Histological Events and Molecular Changes in Excisional Wound Healing of Diabetic DB/DB Mice, J. Surg. Res. 238 (2019) 186–197.
[77] J.L. Burgess, W.A. Wyant, B. Abdo Abujamra, R.S. Kirsner, I. Jozic, Diabetic Wound-Healing Science, Med. (Kaunas.) 57 (2021) 1072.
[78] G. Zhao, P.C. Hochwalt, M.L. Usui, R.A. Underwood, P.K. Singh, G.A. James, P. S. Stewart, P. Fleckman, J.E. Olerud, Delayed wound healing in diabetic (db/db) mice with Pseudomonas aeruginosa biofilm challenge: a model for the study of chronic wounds, Wound Repair. Regen. 18 (2010) 467–477.
[79] H. Li, X. Chen, K. Ren, L. Wu, G. Chen, L. Xu, Qualitative study on diabetic cutaneous wound healing with radiation crosslinked bilayer collagen scaffold in rat model, Sci. Rep. 13 (2023) 6399.
[80] B.K. Nahak, J. Roy Chowdhury, M.K. Sharma, A. Khan, A. Ganguly, U.K. Singh, P. Parashar, C.-H. Kuan, N.-C. Cheng, Z.-H. Lin, Advancements in multimodal approaches for enhanced wound healing: From chemical to physical strategies, Mater. Today 88 (2025) 1087–1125.
[81] S.C. Chuang, S.A. Yu, P.C. Hung, A.E. Chuang, J.W. Liang, L. Rethi, C.K. Chen, H. W. Fang, H.T. Nguyen, H.T. Lu, Transformative lactera-polypyrrole@carrageenan microparticles leveraging NIR for skin regeneration and stress relief, Int. J. Biol. Macromol. 316 (2025) 144436.
[82] C. Goudot, A. Coillard, A.C. Villani, P. Gueguen, A. Cros, S. Sarkizova, T.L. Tang-Huau, M. Bohec, S. Baulande, N. Hacohen, S. Amigorena, E. Segura, Aryl Hydrocarbon Receptor Controls Monocyte Differentiation into Dendritic Cells versus Macrophages, Immunity 47 (2017) 582–596.e586.
[83] R. Huchzermeier, E.P.C. van der Vorst, Aryl hydrocarbon receptor (AHR) and nuclear factor erythroid-derived 2-like 2 (NRF2): An important crosstalk in the gut-liver axis, Biochem. Pharmacol. 233 (2025) 116785.
[84] D. Lei, L. Liao, T. Qin, X. Guan, K. Duan, Z. Gao, W. Jin, M. Yin, K. Zhang, Y. Liu, Y. Chen, H. Gao, J. Li, F. Huang, W. Liu, C. Xia, B. Wang, H. Huang, S. Lv, Q. Zhi, J. Huang, M. Gao, J. Lu, Reprogramming Lung Redox Homeostasis by NIR Driven Ultra-Small Pd Loaded Covalent Organic Framework Inhibits NF-κB Pathway for Acute Lung Injury Immunotherapy, Adv. Sci. 12 (2025) 2413697.
[85] Y. Wu, J. Che, P. Jia, Y. Ma, Q. Han, X. Wang, L. Fu, H. Dou, Y. Zheng, Near-infrared light-triggered polypyrrole promotes C2C12 cell differentiation and inhibits TNF-α induced myotube atrophy, Cell. Signal. 100 (2022) 110463.
[86] F. Chen, Y. Qiu, J. Liu, NIR responsive nanosystem based on upconversion nanoparticle-engineered bacteria for immune/photodynamic combined therapy with bacteria self-clearing capability, J. Colloid Interface Sci. 678 (2025) 583–594.
[87] Z. Ji, D. Yang, H. Wang, Z. Sun, L. Song, X. Liu, H. Wang, Y. Chen, H. Cao, Y. You, G. Jiao, A NIR-Responsive MXene-Based Hydrogel with Antibacterial and Repair-Promoting Functions for Treating Infected Wounds, Adv. Funct. Mater. n/a (2025) e25674.
[88] W.-T. Liao, C.-H. Hung, S.-S. Liang, S. Yu, J.-H. Lu, C.-H. Lee, C.-Y. Chai, H.-S. Yu, Anti-Inflammatory Effects Induced by Near-Infrared Light Irradiation through M2 Macrophage Polarization, J. Invest. Dermatol. 141 (2021) 2056–2066, e2010.